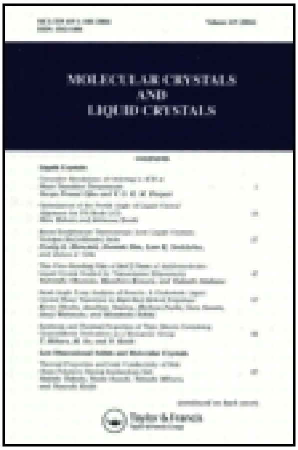

Molecular Crystals and Liquid Crystals
Publication details, including instructions for authors and subscription information:
http://www.tandfonline.com/loi/gmcl20

Optical Tweezers System by Using a Liquid Crystal Optical Device

Marenori Kawamura [a], Mao Ye [a] & Susumu Sato [a]
[a] Department of Electrical and Electronic Engineering, Akita University, Tegtagakuen-cho, Akita, Japan

Version of record first published: 22 Sep 2010

Mol. Cryst. Liq. Cryst., Vol. 478, pp. 135/[891]–142/[898], 2007

ISSN: 1542-1406 print/1563-5287 online
DOI: 10.1080/15421400701681455

Optical Tweezers System by Using a Liquid Crystal Optical Device

Marenori Kawamura
Mao Ye
Susumu Sato
Department of Electrical and Electronic Engineering,
Akita University, Tegtagakuen-cho, Akita, Japan

We propose an optical tweezers system for controlling three-dimensional (3D) manipulation and rotation of microscopic particles by using a liquid crystal (LC) device with three functions of anamorphic lens properties in addition to both variable-beam focusing and deflection properties. The trapped particles suspended in the water can be moved in 3D directions and also be rotated by applying voltages to the LC lens without the use of any mechanically moving parts.

Keywords: anamorphic lens property; beam deflection; laser manipulation; liquid crystal optical device; optical tweezers; variable-focusing

1. INTRODUCTION

Optical tweezers or optical traps are powerful tools for manipulating micrometer-size dielectric particles and biological cells by using a tightly focused laser light beam [1–3]. The optical manipulation of the trapped particles requires certain mechanical procedures for moving the focusing point of an objective lens and scanning the laser beam.

Since a liquid-crystal (LC) material has high electrical and optical anisotropies, the LC molecules can easily be reoriented by an external electric field and, thus, its optical properties can be controlled. Not only flat-panel display devices but some applications of small active optical components such as LC lenses [4–10], gratings [11], light beam steering [12] and other optical devices that use the LC materials have been reported.

Address correspondence to Marenori Kawamura, Department of Electrical and Electronic Engineering, Akita University, 1-1 Tegtagakuen-cho, Akita 010-8502, Japan. E-mail: Kawamura@ipc.akita-u.ac.jp

Previously, we reported an optical tweezers system for controlling three-dimensional (3D) manipulation of microscopic particles by using an LC optical device with variable focusing of laser-beam and deflection properties [13]. The position of the trapped polymer ball (diameter: 11 μm) could be controlled in 3D directions.

In this work, we propose a novel optical tweezers system by using an LC lens fabricated with eight-divided circularly hole-patterned electrodes, which has electrically tunable special functions of variable-beam focusing, deflection and anamorphic lens properties. The trapped microscopic and slender glass objects dispersed in the water can be moved in 3D directions and also rotated clockwise and anticlockwise in transverse directions by adjusting an appropriate voltages to the divided electrodes of the LC lens.

2. EXPERIMENTAL

The instrumentation of an optical tweezers system that uses the LC lens with laser beam control functions is schematically shown in Figure 1. An expanded laser beam at a wavelength of 532 nm from the laser light source (Verdi^{TM}, Coherent Japan Co.) is collimated using two convex lenses L_1 ($f = 40$ mm) and L_2 ($f = 100$ mm), passes through the LC lens and objective lens (×40, NA = 0.45) of microscope.

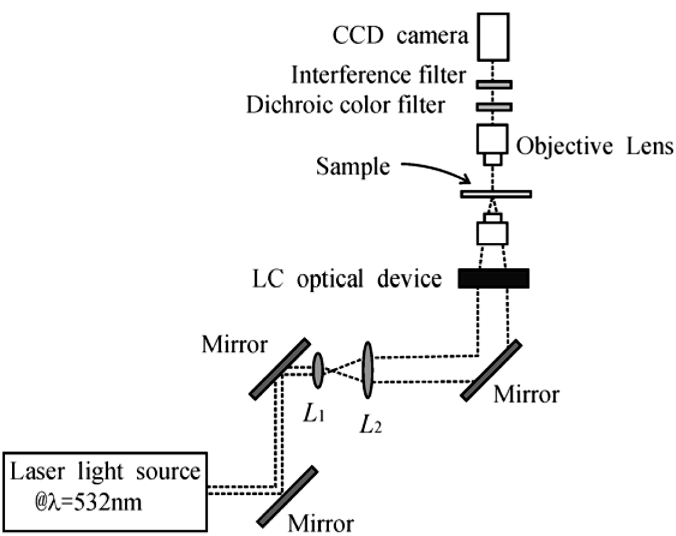

FIGURE 1 Schematic diagram of an optical tweezers system based on an LC lens.

The slender glass rod particles of 30–50 μm length at a diameter of 11 μm are suspended in the distilled water and used as a test sample. The test sample is placed on the center of the slide glass substrate, illuminated by white light source and observed using microscope with an objective lens (×20) and a charge-coupled device (CCD) array camera. A dichroic color filter at a wavelength of 550–750 nm and an interference filter at a center wavelength of 589 nm are used to protect the CCD array camera from the very intense laser beam. Only the imaging light passes through the filters; the trapped particles can be observed by using the CCD array camera.

Figures 2(a) and 2(b) show schematic diagrams of top and side view of the LC lens with eight-divided circularly hole-patterned electrodes for capturing and controlling microscopic objects. The LC lens was fabricated with the hole-patterned electrodes on one glass substrate by a photolithographic technique after depositing aluminum thin films on the glass substrate (1.1 mm thick). The aperture diameter of the hole-patterned electrodes was 6.7 mmϕ. The surfaces of the rear side of the hole-patterned region and an indium tin oxide (ITO) electrode of another substrate were coated with polyimide films, and rubbed unidirectionally. Two substrates were overlapped with polymer ball

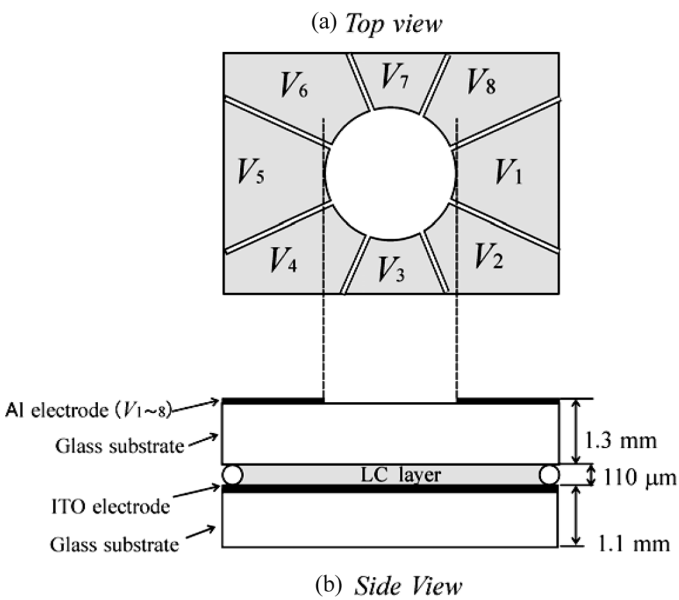

FIGURE 2 Schematic diagram of an LC lens with eight-divided circularly hole-patterned electrodes.

spacers at a diameter of 110 μm. A nematic LC material (E44, Merck) with a positive dielectric anisotropy was injected into the empty cell. Each voltage of V_1–V_8 to the eight-divided electrodes can be applied independently. The LC lens properties are observed by an interference method using a helium-neon laser beam under crossed polarizers [9].

3. RESULTS AND DISCUSSION

Figures 3(a)–3(d) show the interference fringe patterns of the circularly hole-patterned region at several voltages to the eight-divided electrodes; (a) $V_1 = V_5 = 45\,V_{rms}$, $V_2 = V_4 = V_6 = V_8 = 64\,V_{rms}$, $V_3 = V_7 = 90\,V_{rms}$, (b) $V_2 = V_6 = 45\,V_{rms}$, $V_1 = V_3 = V_5 = V_7 = 64\,V_{rms}$, $V_4 = V_8 = 90\,V_{rms}$, (c) $V_3 = V_7 = 45\,V_{rms}$, $V_2 = V_4 = V_6 = V_8 = 64\,V_{rms}$, $V_1 = V_5 = 90\,V_{rms}$, (d) $V_4 = V_8 = 45\,V_{rms}$, $V_1 = V_3 = V_5 = V_7 = 64\,V_{rms}$, $V_2 = V_6 = 90\,V_{rms}$ under crossed polarizers. The interference patterns are composed of

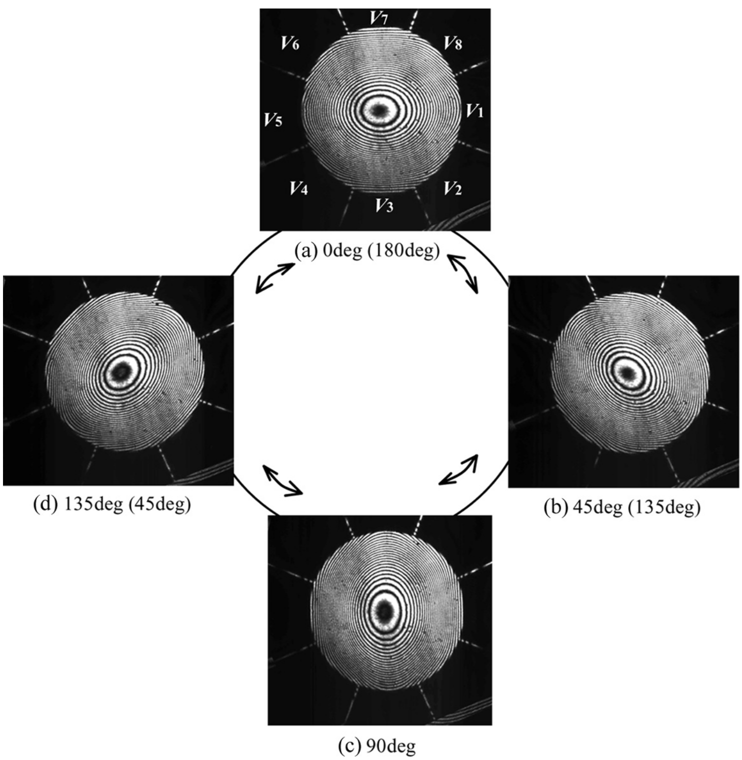

FIGURE 3 Interference fringe patterns of the LC lens under crossed polarizers.

elliptical fringes and the direction of major axis of the fringes can be rotated from 0° to 180° by 45° with adjusting the control voltage to each electrode. The fringe distributions exhibit good symmetrical properties with respect to the major and minor axes. When the same voltage is applied to each divided electrode, almost circular fringes can be observed and the LC cell has convex lens properties.

From the observed interference patterns, the phase profile distributions of a linearly polarized incident light along the major axis and minor axis are obtained as shown in Figure 4. The open and solid circles represent the experimental results from the interference patterns shown in Figure 3(b) and the solid lines represent quadratic fitting. It is seen that the phase profiles have quadratic distributions of the hole-patterned region along the major or minor axes from about $-2.5\,\text{mm}$ to $+2.5\,\text{mm}$. The lens powers for two axes can also be estimated to be about $5.3\,\text{m}^{-1}$ and $3.3\,\text{m}^{-1}$, respectively. Then an anamorphic lens with the large astigmatic aberration property can be attained. The lens power increases as increasing the applied voltage to each electrode. Since the phase distributions tend to deviate from the quadratic distributions at outside the area of $\pm 2.5\,\text{mm}$, both spherical aberrations along the major and minor axes increase. We will discuss these aberration properties of the LC device in more detail elsewhere.

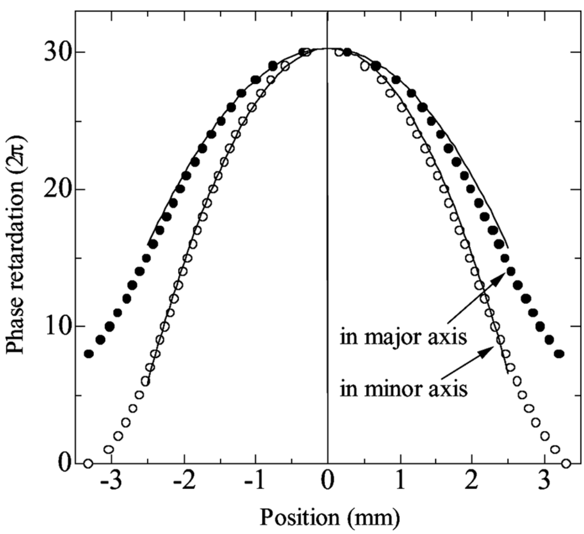

FIGURE 4 Phase retardations of the LC lens along major axis and minor axis. ($V_2 = V_6 = 45\,\text{V}_{\text{rms}}$, $V_1 = V_3 = V_5 = V_7 = 64\,\text{V}_{\text{rms}}$, $V_4 = V_8 = 90\,\text{V}_{\text{rms}}$).

Figures 5(a)–5(d) show the laser manipulation images of the trapped glass rod particles dispersed into the water. Adjusting the control voltage to each electrode of the LC lens, the laser beam can be focused with any profile of elliptical cross section. The elliptical beam, that was shown in Figure 4, was used to apply a torque to the trapped glass rod particles. The slender object aligns along the major axis of the elliptically shaped laser beam spot. The trapped particles can be rotated clockwise or anticlockwise during the application of the rotating control voltage to the divided electrodes of the LC lens.

Figure 6 shows the shift of the trapped particle caused by the laser beam deflection with respect to the applied voltage V_4 shown in Figure 2. The trapping laser spot is deflected in transverse directions so as not to deform focusing properties by changing and adjusting the applied voltage to the divided electrode. It is seen that the position of the trapped particle can be shifted and the variable range of the shift is estimated to be about $\pm 15\,\mu$m.

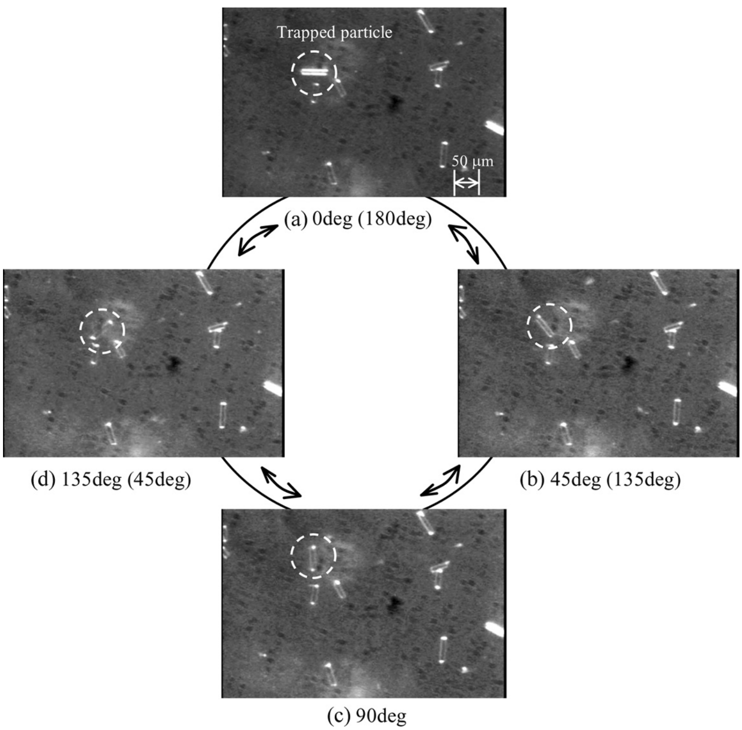

FIGURE 5 Images of the optically trapped glass rod particle observed using a CCD array camera.

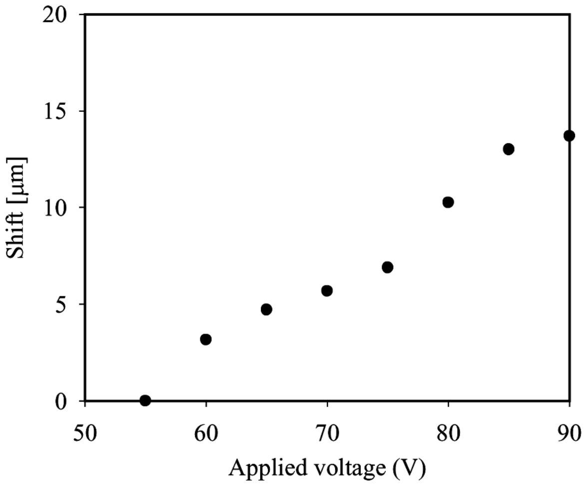

FIGURE 6 Shift of the trapped glass rod particle in the transverse directions.

4. CONCLUSION

We have proposed a laser tweezers system with 3D controllable and rotatable trapping by using an LC lens with eight-divided circularly hole-patterned electrodes. Since the LC lens has electrically controlling functions such as a beam-steering, variable focal length and anamorphic lens property, the circularly and/or elliptically focused laser spot in the trapped area can be realized by adjusting the control voltage to the LC lens. Therefore, the trapped microscopic slender particles can be controlled in 3D positions and also be rotated freely in the transverse direction.

REFERENCES

[1] Ashkin, A., Dziedzic, J. M., & Yamane, T. (1987). *Nature*, *330*, 769.
[2] Wirght, W. H., Jsonek, G., & Berns, M. W. (1994). *Appl. Opt.*, *33*, 1735.
[3] Cojoc, D., Emiliani, V., Ferrari, E., Malreanu, R., Cabrini, S., Proietti, Z. R., & Fabrizio, E. D. (2004). *Jpn. J. Appl. Phys.*, *43*, 3910.
[4] Sato, S. (1979). *Jpn. J. Appl. Phys.*, *18*, 1679.
[5] Nose, T. & Sato, S. (1989). *Liq. Cryst.*, *5*, 1425.
[6] Sato, S. (1999). *Opt. Rev.*, *6*, 471.
[7] Ye, M. & Sato, S. (2002). *Jpn. J. Appl. Phys.*, *41*, L571.
[8] Wang, B., Ye, M., Honma, M., Nose, T., & Sato, S. (2002). *Jpn. J. Appl. Phys.*, *41*, L1232.
[9] Ye, M., Wang, B., & Sato, S. (2004). *Appl. Opt.*, *43*, 6407.

[10] Ye, M. & Sato, S. (2003). *Opt. Comm.*, *225*, 277.
[11] He, Z., Nose, T., & Sato, S. (1998). *Opt. Eng.*, *37*, 2885.
[12] Masuda, S., Takahashi, S., Nose, T., Sato, S., & Ito, H. (1997). *Appl. Opt.*, *36*, 4772.
[13] Kawamura, M., Ye, M., & Sato, S. (2005). *Jpn. J. Appl. Phys.*, *44*, 6098.